ChemistrySelect

Research Article
doi.org/10.1002/slct.202302266

Chemistry Europe
European Chemical Societies Publishing

www.chemistryselect.org

Cavity Size Effects on the Adsorption of CO_2 on Pillar[n]arene Structures: A Density Functional Theory Study

Quoc Duy Ho*[a] and Eva Rauls[a]

Carbon dioxide (CO_2) is the main greenhouse gas that contributes to the global warming. Therefore, CO_2 adsorption is very urgent in the fight to limit global warming below 1.5 degrees Celsius. In this report, the interaction between CO_2 with different structures of pillar[n]arene (P[n]A) is studied by using DFTB and DFT calculations, in order to understand the effect of P[n]A (with n = 4, 5, and 6) cavity sizes on CO_2 adsorption. The P[n]A structures physisorb CO_2 at three principally different positions called cavity-in, top-in, and top-out. The adsorbed CO_2-cavity-in at P[4]A has the highest binding energy. The adsorbed CO_2 at the other positions has similar binding energies on P[4]A, P[5]A, and P[6]A, because hydrogen bonding plays a major role for the interaction at the hydroxyl group. The number of CO_2 molecules that can be adsorbed at the cavity site depends on the cavity size of P[n]A. The bigger the cavity site, the larger the number of CO_2 molecules that can be adsorbed before saturation is achieved. We also observed that the adsorbed CO_2 molecules can interact with each other, leading to an increase of the binding energy and highlighting the promising CO_2 capture capabilities of P[n]A structures.

Introduction

Carbon dioxide is a natural gas present in the Earth's atmosphere. However, the intensification of CO_2 concentration from industrial activities causes global warming. Therefore, reducing this greenhouse gases by carbon capture and sequestration (CCS) procedures has become more and more significant. The CCS procedure begins with capturing CO_2 from power plants and then compressing the captured CO_2 before transporting them to permanent storage sites. In the CCS schemes, capturing CO_2 is the most expensive process, therefore, many materials such as metal oxides,[1–3] alloys,[4,5] metal organic frameworks (MOF),[6–8] zeolites,[9,10] and soft organic frameworks (SOF)[11–13] have been studied to reduce the cost of the process. Amongst these materials, SOF materials have recently attracted a lot of attention because of their promising property of host-guest interactions with CO_2.

P[n]A is a macrocycle compound, made from *n*-hydroquinone units (with $n = 4, 5, 6, 7 \ldots$). The units are linked by methylene bridges at para positions. Since 2008, when P[5]A was first synthesized by Ogoshi *et al.*,[14] it has become a very promising material for CO_2 capturing applications. P[5]A can be synthesized with a yield of 71 % by using commercially available reagents,[15] it is chemically and thermally stable,[13] the functional groups of P[5]A can adsorb CO_2 at both the cavity site and functional groups.[16] P[5]A is highly CO_2 selective adsorption over CH_4 and N_2.[13,16] Last but not least, P[5]A is water-soluble, such that it can be easily transferred to already existing industrial CO_2 absorption plants.

In addition to P[5]A, the pillar structure with 6–10 arene units (P[6]A, P[7]A, P[8]A, P[9]A, and P[10]A) were synthesized successfully. However, due to their high yields, only P[5]A and P[6]A have been widely used so far. Most of the studies of P[n]A have, thus, focused on P[5]A, and P[6]A structures. In comparison to P[6]A, P[5]A has a smaller cavity size (6.7 Å vs 4.7 Å diameters), they are both larger than the kinetic diameter of CO_2 (3.3 Å). Even though there have been many studies of CO_2 adsorption of P[n]A materials,[13,17–20] the effect of P[n]A cavity sizes on CO_2 adsorption has not yet been understood in detail. Here, we present our computational studies on the adsorption of CO_2 on various P[n]A to understand how the cavity size affects the CO_2 adsorption efficiency and for which *n* of the P[n]A is optimally efficient.

Computational Calculation Details

Our calculations were carried out using the self-consistent charge density-functional-based tight-binding (SCC-DFTB) method[21–23] implemented in the DFTB + 22.1 code.[24] The DFTB calculations are in good agreement with the results from density functional theory (DFT) method but at much lower cost,[25] this was confirmed for the pillar[5]arenes system in our previous study.[16] We use the mio-1-1 basis set in our calculations.[22] The electron core is frozen. *2s*, *2p*, and *1s* valence orbitals are used for carbon, oxygen, and *1s* for hydrogen, respectively. The *SimpleDftD3* dispersion correction scheme was applied to correct the van der Waals interaction. The structures with a vacuum space of at least 15 Å to avoid the periodic image interaction. A convergence condition of 10^{-4} eV was applied to the self-consistent electronic energy, with the relaxation calculation, the optimization was stopped for maximum forces

[a] *Dr. Q. D. Ho, Prof. E. Rauls*
Department of mathematics and physics, Universitetet i Stavanger, Stavanger, Norway 4021
E-mail: duy.hoquoc@uis.no
Homepage: https://www.uis.no/nb/profile/quoc-duy-ho

below 10^{-4} eV/A. The Γ k-point approximation[26] are used in all calculations.

VASP 5.4.4 and the projector augmented wave method[27–29] was used for the DFT calculations and the zero-phonon energy (ZPE) correction. In our VASP calculations, PBE exchange-correlation was used with a plane wave cut-off of 400 eV. The van der Waals contributions were included by using the DFT-D3 scheme.

Results and Discussion

We studied the adsorption of CO_2 gas molecules on P[4]A, P[5]A, and P[6]A to understand how the cavity size affects CO_2 adsorption and how many CO_2 molecules can be adsorbed by a single P[n]A. P[5]A and P[6]A were chosen because they can be synthesized with high yields, 71% and 87%, respectively.[14,30] Despite both P[4]A and P[7]A are the next size structures of P[5]A and P[6]A, only P[4]A was selected for this study because it is more stable than that P[7]A: 1.10 kcal/mol/monomer in comparison to 1.32 kcal/mol/monomer.[31] In addition, as discussed in the previous report, the main driving force that attracts CO_2 to the cavity site of P[5]A is the π-π interaction between the CO_2 and one or several benzene rings of P[5]A.[16] Since the cavity size of P[4]A is much smaller than that of P[7]A, the effect of π-π interaction between the adsorbed CO_2 and the benzene rings plays an even more important role in P[4]A than in P[7]A.

The adsorption energies have been calculated as equation (1) below:

$$E_{ads} = E_{P[n]As+CO_2} - \left(E_{P[n]As} + E_{CO_2}\right) \quad (1)$$

Where E_{ads}, $E_{P[n]As+CO_2}$, $E_{P[n]As}$, and E_{CO_2} are the adsorption energy, the total energy of P[n]A ($n=4$, 5, 6) with the adsorbed CO_2 molecule, P[n]A total energy, and isolated CO_2 molecule energy, respectively. The more favorable the adsorption, the higher negative value we get.

The binding energies of CO_2 in P[n]A are presented in Table 1. It is important to note that the results obtained through DFTB calculations demonstrate very good agreement with those obtained from DFT methods. Table 1 indicates that the impact of ZPE correction on the binding energies of CO_2 in P[n]A is relatively small. In addition, the calculated results with DFT method for 2 adsorbed CO_2 (1 cavity-in and 1 top-in) at P[4]A also show a very small change of binding energy (−0.03 eV) when considering the ZPE correction. Our calculated results of ZPE correction align very well with the findings of a previous study conducted by Govender *et al.*,[32] which suggested that the inclusion of ZPE correction only leads to a very slight change in the adsorption energy and does not alter the trends. Therefore, we have not considered the ZPE correction in our calculations of the adsorption energy.

Our previous study showed that P[5]A can adsorb a CO_2 molecule at the cavity site (so-called CO_2-cavity-in) and in two different arrangements at one of the –OH functional groups (so-called CO_2-top-in and CO_2-top-out).[16] Figure 1 shows the adsorbed CO_2-cavity-in molecule at P[4]A (Figure 1a), P[5]A (Figure 1b), and P[6]A (Figure 1c). The adsorbed CO_2-cavity-in is parallel to the axis of P[n]A (the dashed blue line). The calculated adsorption energy is shown in Table 1. The adsorbed CO_2-cavity-in at P[4]A has the highest adsorption energy, the adsorption energy in P[6]A is the smallest. The difference of the adsorption energy between P[4]A, P[5]A, and P[6]A can be explained as follows: Because of the π-electron-rich cavity of P[n]A,[33,34] CO_2 is adsorbed at the cavity site mainly due to the π-π interaction between CO_2 and the aromatic rings. Due to the small cavity site of P[4]A, the π-π interaction is stronger in P[4]A than P[5]A or P[6]A. In the case of P[5]A and P[6]A, CO_2 interacts mainly with two adjacent benzene rings. In P[4]A, however, CO_2 interacts with all 4 benzene rings. The distance of CO_2 from the other benzene rings of P[5]A is slightly shorter than in P[6]A, so that the adsorption energy of P[5]A is slightly higher. The symmetric structure and the small cavity size of P[4]A causes that CO_2 can interact with all 4 benzene rings equally and locates exactly in the middle of P[4]A (3.14 Å to each benzene ring). Due to the interaction with more than 1 benzene ring, this distance in P[4]A (3.14 Å to 4 benzene rings), and in P[6]A (3.0 to 2 benzene rings) is shorter than between CO_2 and benzene T-C_6H_6 of Chen *et al.* (3.35 Å).[35]

Besides the adsorption at the cavity site, CO_2 can also adsorb by hydrogen bonding to the hydroxyl groups on top or on bottom of the P[n]A. Figure 2 shows the CO_2-top-in and CO_2-top-out conformations at P[4]A (Figure 2a), P[5]A (Figure 2b), and P[6]A(Figure 2c). Table 1 lists up the adsorption energies of these conformations with around 0.22 eV and 0.17 eV for the top-in and the top-out conformations, respectively. Since hydrogen bonding plays a major role in the adsorption at the top-in and top-out conformations, the size of the cavity turns out to be nearly irrelevant the adsorption energies at these conformations.

In short, the binding energy between the adsorbed CO_2-cavity-in decreases with increasing cavity size. The pillar structure with 4 arene monomers has the strongest interaction with CO_2 at the cavity site. CO_2 adsorption at the –OH groups are not affected by the cavity size. Next, we will turn to the question what happens when more than one CO_2 molecule

Table 1. CO_2 adsorption energies (in eV) for the three different structures (cf. Figure 1). The results of DFTB and DFT calculations obtained with the DFTB+ and VASP code, respectively.

Position	P[4]A			P[5]A			P[6]A		
	DFTB	DFT	DFT+ZPE	DFTB	DFT	DFT+ZPE	DFTB	DFT	DFT+ZPE
Cavity-in	−0.53	−0.50	−0.51	−0.35	−0.33	−0.36	−0.29	−0.27	−0.28
Top-in	−0.23	−0.21	−0.23	−0.22	−0.23	−0.25	−0.22	−0.20	−0.23
Top-out	−0.17	−0.16	−0.18	−0.17	−0.16	−0.19	−0.16	−0.17	−0.18

Research Article
doi.org/10.1002/slct.202302266

Chemistry Europe
European Chemical Societies Publishing

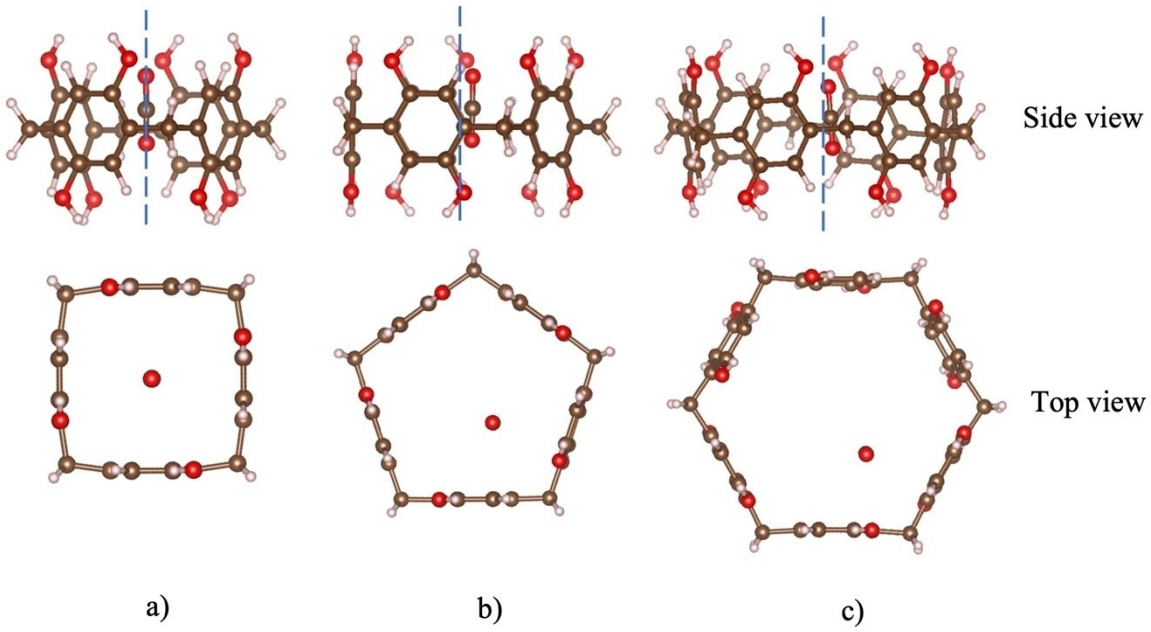

Figure 1. Atomic structures of adsorbed CO_2-cavity-in conformation at a) P[4]A, b) P[5]A, and c) P[6]A.

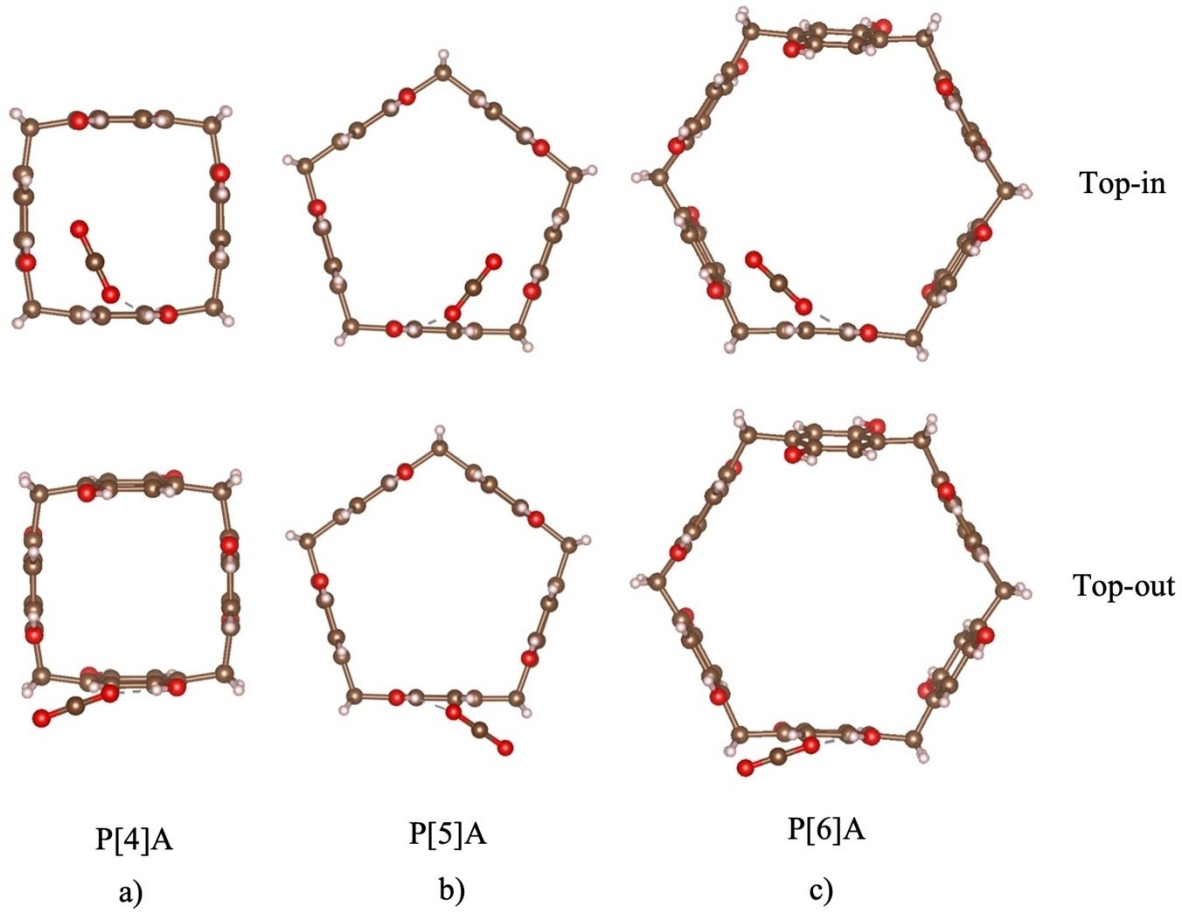

Figure 2. Top views of P[4]A, P[5]A, and P[6]A with the adsorbed CO_2 at top-in and top-out conformations.

approaches a P[n]A. How many CO_2 molecules can the P[n]A bind and in which configurations?

Figure 3a shows the initial positions of P[4]A with 2 CO_2 molecules placed at the cavity site parallel to each other and to the axis of P[4]A (the dash blue line). After relaxation (Figure 3b), one CO_2 molecule is captured in the middle of the P[4]A cavity site, similar to the single CO_2-cavity-in position (Figure 1a). The other CO_2 adsorbs via hydrogen bonding at the hydroxyl group. Figure 3b shows that the 2 adsorbed CO_2 molecules' positions are aligned so that the O atom of the CO_2-cavity-in points toward the C atom of the CO_2-top-in. Because of the difference in electronegativity of C and O atoms (2.55 and 3.44, respectively), the electron-rich O of the adsorbed CO_2-cavity-in attracts the electron-depleted C of the CO_2-top-in. This interaction causes the adsorbate with two CO_2 molecules in Figure 3b has a higher binding energy than two separated CO_2 molecules at cavity-in and top-in conformations, -0.82 eV vs -0.52 eV $+(-0.23$ eV$) = -0.75$ eV, respectively. This emphasizes the advantage of using P[n]A in capturing CO_2. The first CO_2 adsorbed at the cavity-in conformation increases the CO_2 uptake ability of the hydroxyl groups of P[n]A.

In the above calculations, we started with two CO_2 molecules at the cavity-in conformation. After relaxation, only one CO_2 molecule can be captured at the cavity-in conformation of P[4]A structure. The question arises here that how many CO_2 molecules can be captured at the cavity-site of P[5]A and P[6]A? To answer this question we have run numerous calculations, placing increasing numbers of CO_2 molecules parallel to the axis of P[5]A and P[6]A and then relaxing the structures. Figure 4 shows the conformations of P[5]A and P[6]A with multiple CO_2 molecules after relaxation. We find that P[5]A can adsorb three CO_2 molecules at the cavity-in conformation. When the 4th CO_2 molecule is added to the cavity site of P[5]A, the structure ends up with three CO_2 at the cavity-in conformation and the 4th CO_2 adsorbed at –OH group (Figure 4a). In the case of P[6]A, 5 CO_2 molecules can be adsorbed in the cavity-in conformation, the 6th CO_2 molecule binds to the –OH group (Figure 4b).

When only one CO_2 molecule is located at the cavity site of P[n]A, the CO_2-cavity-in interacts equally with the aromatic rings of P[n]A. Therefore, the CO_2-cavity-in is parallel to the axis. However, in the case of several adsorbed CO_2 molecules at the cavity-in conformation (Figure 4), the CO_2-cavity-in molecules interact not only with P[n]A but also with each other. The interactions rotate the CO_2 molecules slightly, such that the adsorbed CO_2-cavity-in molecules are no longer parallel to the axis of P[n]A. The C atom points toward the O atom of the nearest CO_2 molecule and keeps the distances between 2 CO_2 molecules around 2.7 Å. It can be seen from Figure 4 that the C of a CO_2 molecule tends to point toward an O of the nearest CO_2 neighbor due to the electronegativity difference between C and O. These interactions increase the binding energies per molecule of CO_2 molecules to P[5]A, and P[6]A. More specifically, the binding energy of 4 CO_2 molecules in P[5]A (Figure 4a) is -1.37 eV, thus a little higher than $3*(-0.35)+(-0.22) = -1.27$ eV (3 CO_2-cavity-in + 1 CO_2-edge-in). In case of P[6]A (Figure 4b), 6 CO_2 bind with -1.95 eV in comparison to $5*-(-0.29)+(-0.22) = -1.67$ eV (5 CO_2-cavity-in + 1 CO_2-edge-in) in the case of 6 CO_2 adsorbed in P[6]A.

Table 2 shows the number of CO_2 molecules that can be adsorbed by P[n]A. The number of adsorbed CO_2 molecules is the total number of the adsorbed CO_2 molecules at the cavity-in and the top-in conformations (Figure 5). The number of CO_2 molecules which can be adsorbed in the cavity of P[n]A

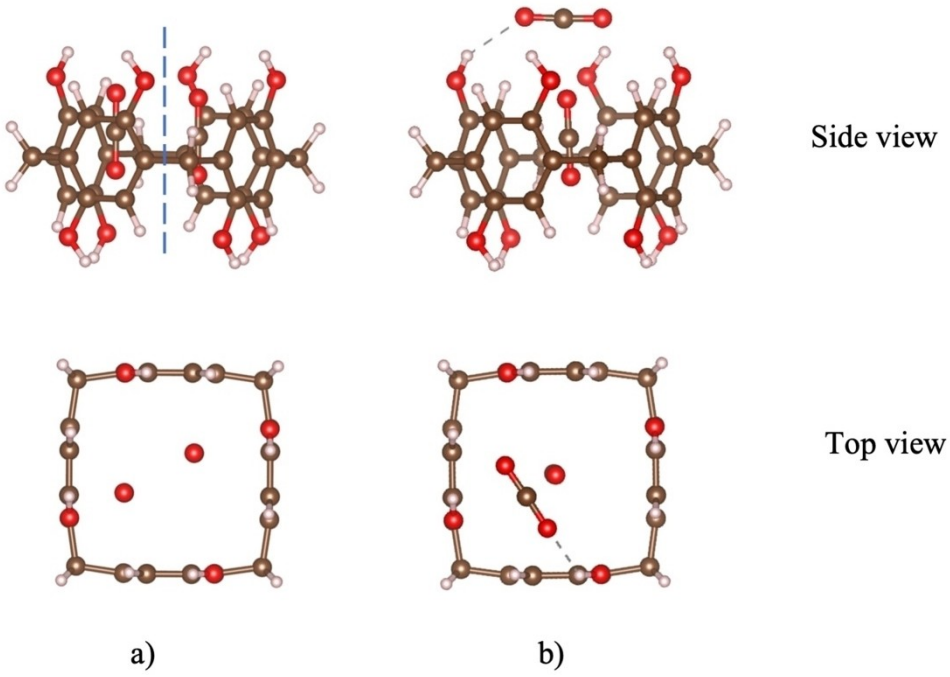

Figure 3. a) Initial positions of 2 CO_2 molecules at the cavity site of P[4]A, b) Optimized adsorption structure obtained from the initial arrangement in Figure a.

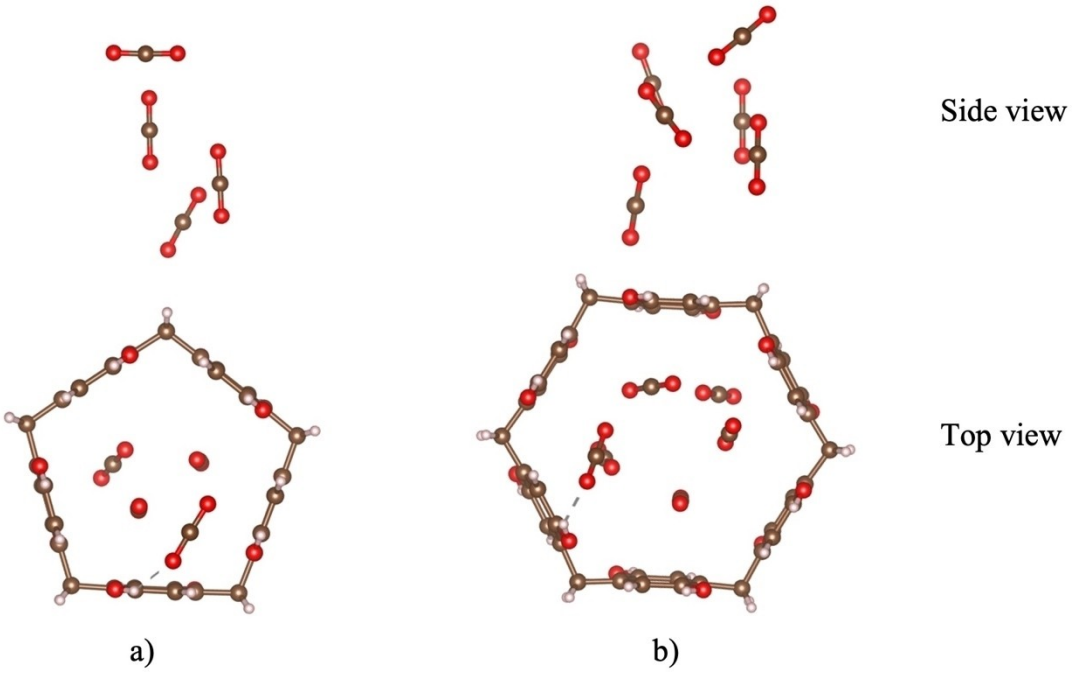

Figure 4. Optimized adsorption structures of a) P[5]A with 4 CO_2 molecules, and b) P[6]A with 6 CO_2 molecules. In the side view, the structures are shown without P[5]A and P[6]A for better visibility.

Table 2. The number of CO_2 molecules adsorbed by P[4]A, P[5]A, and P[6]A.

P[n]A structure	Total number of adsorbed CO_2 molecules	Number of adsorbed CO_2 molecules in the cavity	Number of adsorbed CO_2 molecules per monomer
n = 4	9	1	2.25
n = 5	13	3	2.6
n = 6	17	5	2.83

increases with the cavity size. P[4]A can bind only one CO_2, P[5]A gets 3 CO_2 molecules, while the number of CO_2 molecules at the cavity site of P[6]A is 5. To compare the efficiency of CO_2 adsorption between P[4]A, P[5]A and P[6]A, we calculated the number of adsorbed CO_2 per arene monomer (the last column of table 2). With 2.83 adsorbed CO_2 molecules per arene monomer, P[6]A is the most favorable CO_2 adsorbent amongst the three investigated P[n]A structures.

Figure 6b illustrates the binding energy per CO_2 molecule when adsorbed by P[4]A (red), P[5]A (orange), or P[6]A (blue). For P[5]A, the binding energy remains relatively constant at around 0.3 eV/molecule from the 1st to the 13th adsorbed CO_2 molecule. However, a notable decrease in binding energy is observed for the 14th, 15th, and 16th adsorbed CO_2 molecules (C atoms depicted in green in Figure 6a). These later adsorbed CO_2 molecules exhibit a binding energy of approximately 0.13 eV each. The diminished adsorption energy can be attributed to the fact that these three CO_2 molecules are introduced into the system through interaction with existing CO_2 molecules only. Consequently, they lack both hydrogen bonding and Lewis acid-base interaction with P[5]A (cf Figure 6a). Similar calculations were conducted for P[4]A and P[6]A, revealing binding energies of approximately 0.3 eV per CO_2 molecule for adsorptions up to 9 and 17 molecules for P[4]A and P[6]A, respectively. Even after having filled up the cavity of the P[n]A completely as well as all available hydrogen bonding sites at the –OH groups, CO_2 adsorption continues through interactions between CO_2 molecules. Binding energies of approximately −0.13 eV per molecule are also observed for P[4]A and P[6]A when an additional set of 3 CO_2 molecules is introduced. It is worth noting that a decrease in binding energy (becoming less negative) per CO_2 molecule is observed when comparing the binding energy of the first adsorbed CO_2 molecule to the subsequently adsorbed ones. For example, P[5]A exhibits a binding energy of −0.35 eV for the first adsorbed CO_2 molecule, while the seventh adsorbed CO_2 molecule has a binding energy of −0.28 eV. This discrepancy can be attributed to the fact that the first CO_2 molecule is adsorbed at the cavity site, whereas the seventh CO_2 molecule is adsorbed at the OH group, resulting in a slightly smaller binding energy.

The continuation of CO_2 adsorption after the saturation of all available adsorption sites at P[n]A is likely contributing to the CO_2 selectivity of P[n]A. As discussed in our previous study,[16] the quadrupole moments, and polarizabilities of CH_4 and N_2 are much weaker than in case of CO_2. It is, thus, after all sites of P[n]A are attached with CH_4 or N_2, the adsorption is likely not to happen because of the weak interaction between CH_4 and CH_4 (or between N_2 and N_2, respectively).

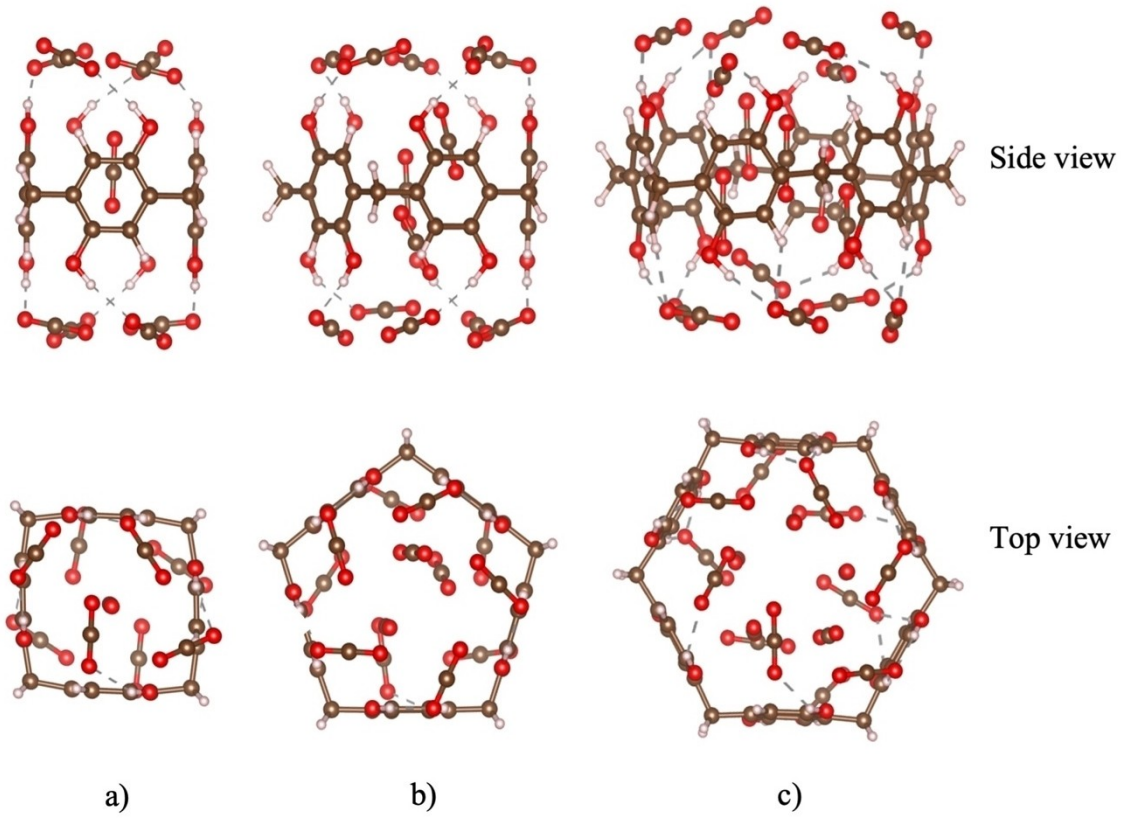

Figure 5. Optimized structures of a) P[4]A with 9 adsorbed CO_2 molecules, b) P[5]A with 13 adsorbed CO_2 molecules, and c) P[6]A with 17 adsorbed CO_2 molecules.

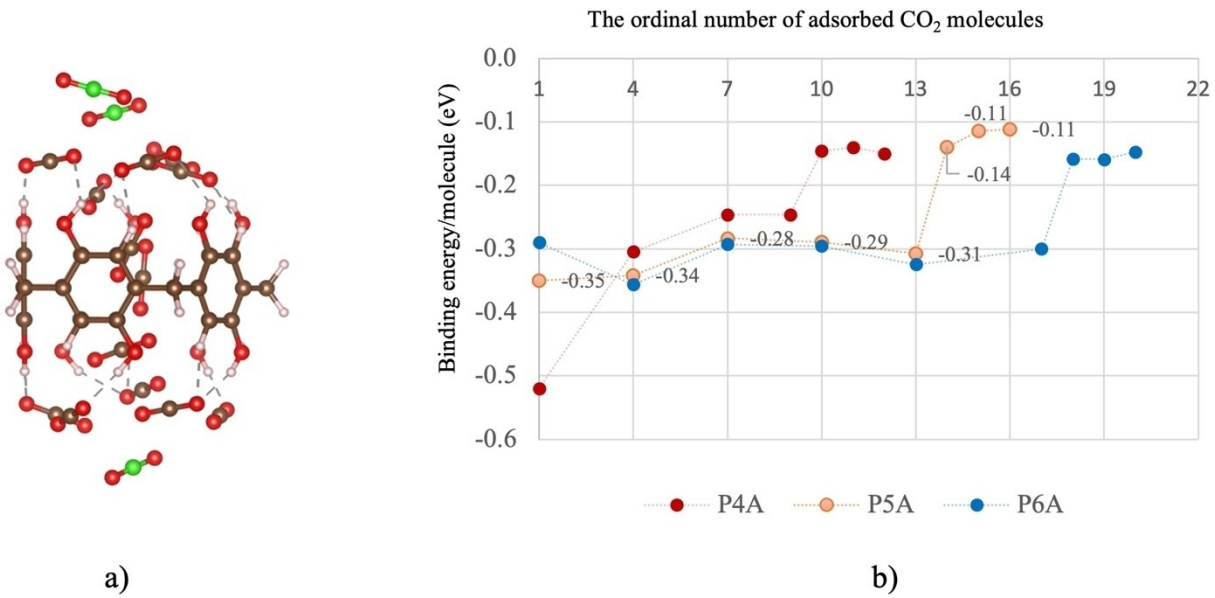

Figure 6. part A) Optimized structures of a) P[5]A with 16 adsorbed CO_2 molecules, part B) binding energy/molecule of adsorbed CO_2 molecules in P[4]A, P[5]A, and P[6]A.

Conclusions

Our findings reveal that the adsorption energies of CO_2 molecules decrease with increasing cavity size, with P[4]A exhibiting the strongest interaction with CO_2 at the cavity site. The interaction between CO_2 and the aromatic rings plays a crucial role. In P[4]A, CO_2 interacts with all four benzene rings, which results in a higher adsorption energy compared to P[5]A

and P[6]A. Hydrogen bonding has been identified as the primary mechanism for adsorption at the top-in and top-out conformations, rendering the cavity size nearly irrelevant in determining the adsorption energies of CO_2 in these positions for all three P[n]A structures. We also examined the adsorption of multiple CO_2 molecules on P[n]A structures. The cavity site of P[4]A can adsorb one CO_2 molecule only, while in the case of P[5]A and P[6]A, 3 and 5 CO_2 molecules can be added to the cavity-in conformation, respectively. When additional CO_2 molecules are introduced, they adsorb at the hydroxyl groups. Interaction between adsorbed CO_2 molecules increases the binding energy, showing another advantage of using P[n]A structures for CO_2 capture. Our study also revealed that CO_2 molecules still can be added to the complex after filling the cavity site due to the weak interaction between CO_2 molecules but with much lower binding energy.

Acknowledgements

The authors greatly acknowledge financial support of the Research Council of Norway within project 324306 in the PETROMAKS 2 program. The calculations with VASP performed on resources provided by Sigma2 - the National Infrastructure for High Performance Computing and Data Storage in Norway (project NN8071K).

Conflict of Interests

The authors declare no conflict of interest.

Data Availability Statement

The data that support the findings of this study are available from the corresponding author upon reasonable request.

Keywords: Ab-initio calculations · Absorption · Nanostructures · Pi interactions · Supramolecular chemistry

[1] B. Feng, H. An, E. Tan, *Energy Fuels* **2007**, *21*, 426–434.
[2] G. A. Mutch, S. Shulda, A. J. McCue, M. J. Menart, C. V. Ciobanu, C. Ngo, J. A. Anderson, R. M. Richards, D. Vega-Maza, *J. Am. Chem. Soc.* **2018**, *140*, 4736–4742.
[3] Q.-L. Tang, Q.-H. Luo, *J. Phys. Chem. C* **2013**, *117*, 22954–22866.
[4] S. A. Rawool, R. Belgamwar, R. Jana, A. Maity, A. Bhumla, N. Yigit, A. Datta, G. Rupprechter, V. Polshettiwar, *Chem. Sci.* **2021**, *12*, 5774–5786.
[5] J. Li, J. Halldin Stenlid, M. T. Tang, H.-J. Peng, F. Abild-Pedersen, *J. Mater. Chem. A* **2022**, *10*, 16171–16181.
[6] J. Yu, L. H. Xie, J. R. Li, Y. Ma, J. M. Seminario, P. B. Balbuena, *Chem. Rev.* **2017**, *117*, 9674–9754.
[7] Q. Wang, D. Astruc, *Chem. Rev.* **2020**, *120*, 1438–1511.
[8] J.-R. Li, Y. Ma, M. C. McCarthy, J. Sculley, J. Yu, H.-K. Jeong, P. B. Balbuena, H.-C. Zhou, *Coord. Chem. Rev.* **2011**, *255*, 1791–1823.
[9] W. Jeong, J. Kim, *J. Phys. Chem. C* **2016**, *120*, 23500–23510.
[10] J. G. Min, K. C. Kemp, H. Lee, S. B. Hong, *J. Phys. Chem. C* **2018**, *122*, 28815–28824.
[11] R. S. Patil, D. Banerjee, C. Zhang, P. K. Thallapally, J. L. Atwood, *Angew. Chem. Int. Ed.* **2016**, *55*, 4523–4526.
[12] J. Lü, C. Perez-Krap, M. Suyetin, N. H. Alsmail, Y. Yan, S. Yang, W. Lewis, E. Bichoutskaia, C. C. Tang, A. J. Blake, R. Cao, M. Schröder, *J. Am. Chem. Soc.* **2014**, *136*, 12828–12831.
[13] L.-L. Tan, H. Li, Y. Tao, S. X.-A. Zhang, B. Wang, Y.-W. Yang, *Adv. Mater.* **2014**, *26*, 7027–7031.
[14] T. Ogoshi, S. Kanai, S. Fujinami, T.-a. Yamagishi, Y. Nakamoto, *J. Am. Chem. Soc.* **2008**, *130*, 5022–5023.
[15] T. Ogoshi, T. Aoki, K. Kitajima, S. Fujinami, T.-a. Yamagishi, Y. Nakamoto, *J. Org. Chem.* **2011**, *76*, 328–331.
[16] Q. D. Ho, E. Rauls, *ChemistrySelect* **2023**, *8*, e202204215.
[17] H. Zhang, C. Li, *RSC Adv.* **2020**, *10*, 18502–18511.
[18] D. Dai, J. Yang, Y.-C. Zou, J.-R. Wu, L.-L. Tan, Y. Wang, B. Li, T. Lu, B. Wang, Y.-W. Yang, *Angew. Chem. Int. Ed.* **2021**, *60*, 8967–8975.
[19] S.-Q. Cheng, X.-Q. Liu, Z.-L. Han, Y. Rong, S.-Y. Qin, Y. Sun, H. Li, *ACS Appl. Mater. Interfaces* **2021**, *13*, 27255–27261.
[20] W. Lin, Z. Cai, X. Lv, Q. Xiao, K. Chen, H. Li, C. Wang, *Ind. Eng. Chem. Res.* **2019**, *58*, 16894–16900.
[21] D. Porezag, T. Frauenheim, T. Köhler, G. Seifert, R. Kaschner, *Phys. Rev. B* **1995**, *51*, 12947–12957.
[22] M. Elstner, D. Porezag, G. Jungnickel, J. Elsner, M. Haugk, T. Frauenheim, S. Suhai, G. Seifert, *Phys. Rev. B* **1998**, *58*, 7260–7268.
[23] G. Seifert, *J. Phys. Chem. A* **2007**, *111*, 5609–5613.
[24] B. Aradi, B. Hourahine, T. Frauenheim, *J. Phys. Chem. A* **2007**, *111*, 5678–5684.
[25] M. Elstner, T. Frauenheim, J. McKelvey, G. Siefert, *J. Phys. Chem. A* **2007**, *111*, 5607–5608.
[26] H. J. Monkhorst, J. D. Pack, *Phys. Rev. B* **1976**, *13*, 5188–5192.
[27] G. Kresse, J. Hafner, *Phys. Rev. B* **1994**, *49*, 14251–14269.
[28] G. Kresse, J. Furthmüller, *Phys. Rev. B* **1996**, *54*, 11169–11186.
[29] G. Kresse, D. Joubert, *Phys. Rev. B* **1999**, *59*, 1758–1775.
[30] T. Ogoshi, N. Ueshima, T. Akutsu, D. Yamafuji, T. Furuta, F. Sakakibara, T.-a. Yamagishi, *Chem. Commun.* **2014**, *50*, 5774–5777.
[31] H. Zuilhof, A. C. H. Sue, J. Escorihuela, *J. Org. Chem.* **2021**, *86*, 14956–14963.
[32] A. Govender, D. Curulla Ferré, J. W. Niemantsverdriet, *ChemPhysChem* **2021**, *13*, 1591–1596.
[33] T. Ogoshi, T. Yamagishi, *Chem. Commun.* **2014**, *50*, 4776–4787.
[34] Y. Wang, G. Ping, C. Li, *Chem. Commun.* **2016**, *52*, 9858–8772.
[35] L. Chen, F. Cao, H. Sun, *Int. J. Quantum Chem.* **2013**, *113*, 2261–2266.

Manuscript received: June 6, 2023